A Journal of the Gesellschaft Deutscher Chemiker
Angewandte Chemie
GDCh
International Edition
www.angewandte.org

Accepted Article

Title: Metal-free Transformations of Nitrogen-oxyanions to Ammonia via Oxoammonium Salt

Authors: Subrata Kundu, Tuhin Sahana, Aditesh Mondal, and Anju B S

To be cited as: *Angew. Chem. Int. Ed.* 10.1002/anie.202105723

Link to VoR: https://doi.org/10.1002/anie.202105723

WILEY-VCH

10.1002/anie.202105723

WILEY-VCH

COMMUNICATION

Metal-free Transformations of Nitrogen-oxyanions to Ammonia *via* Oxoammonium Salt

Tuhin Sahana,[a] Aditesh Mondal,[a] Anju B. S.,[a] and Subrata Kundu*[a]

Abstract: Transformations of nitrogen-oxyanions (NO_x^-) to ammonia impart pivotal roles in sustainable biogeochemical processes. While metal mediated reductions of NO_x^- are relatively well known, this report herein illustrates proton-assisted activations of NO_x^- anions in the presence of electron rich aromatics such as 1,3,5-trimethoxybenzene (TMB–H, **1a**) leading to the formation of oxoammonium salt $[(TMB)_2N^+{=}O][NO_3^-]$ (**2a**) *via* the intermediacy of NO^+. Detailed characterizations including X-ray diffraction, multinuclear (^1H, ^{13}C, ^{15}N) NMR, and HRMS analyses on the metastable species **2a** disclose unambiguous structural and spectroscopic signatures. Oxoammonium salt **2a** exhibits $2e^-$ oxidative reactivity in the presence of oxidizable substrates such as benzyl amine, thiols, and ferrocene. Intriguingly, reaction of **2a** with water affords ammonia. Perhaps of the broader significance, this work reveals a new metal-free route germane to the conversion of NO_x to NH_3.

Nitrogen-oxyanions (NO_x^-), namely nitrate (NO_3^-) and nitrite (NO_2^-), are integral parts of the biogeochemical nitrogen (N) cycle, and play leading roles in fixed-N management relevant to agriculture as well as environment.[1] While ammonium (NH_4^+) can be directly involved in the biosynthesis of proteins and nucleic acids, nitrifying microorganisms present in soil oxidize a significant portion of NH_4^+ to NO_3^-, the most abundant and stable reservoir of fixed-N.[2] Interestingly, assimilatory NO_x^- reductions offer regeneration of NH_4^+ for the incorporation of N into the biomass.[2,3] Furthermore, NO_x^- anions serve as air-stable reservoirs for nitric oxide (NO), a gasotransmitter involved in mammalian physiology.[4] In addition to the inorganic nitrogen-oxyanions, closely related organic molecules such as *O*–nitrites (R–ONOs) and *S*–thionitrites (R–SNOs) are stable reservoirs and circulator of NO, respectively.[5,6]

Owing to the weak RS–NO bond (BDE_{S-N} = ~30 kcal/mol),[6] *S*–thionitrites promptly release •NO along with the generation of disulfide (RS–SR) at ambient temperature. In contrast, RO–NO bond homolysis is slower due to the relatively higher bond dissociation energy (~41 kcal/mol).[7] Interestingly, a number of cogent demonstrations show that RSNOs serve as NO^+, •NO, and NO^- donors in the presence of varied chemical environments.[8] Notably, *O*–nitrites at elevated thermal conditions or in the presence of acid serve as •NO and NO^+ donors, respectively.[9] In contrast to the reactive nature of organic nitrite compounds, NO_x^- anions are relatively inert and requires harsh reaction conditions or transition metals for the activation and reduction (Figure 1A). For instance, nitrate reductase (NAR) employs Mo-dependent active site for the reduction of NO_3^- to NO_2^- ($NO_3^- + 2H^+ + 2e^- \rightarrow NO_2^- + H_2O$) and nitrite reductase (NIR) enzymes include Fe or Cu containing active sites for nitrite reduction ($NO_2^- + 2H^+ + e^- \rightarrow NO + H_2O$).[2,3] Moreover, heme Fe site in cytochrome *c* nitrite reductase (CcNIR) mediates six electron reduction of nitrite to ammonia.[3]

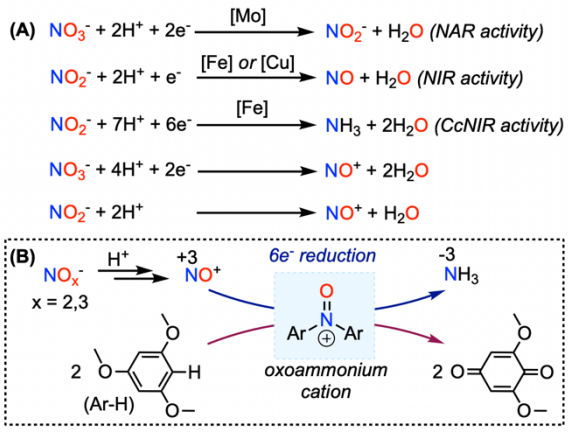

Figure 1. (A) Representative routes for the reductions of nitrite and nitrate anions. (B) Overview of this work.

Stimulated by the metalloenzyme active sites for nitrate and nitrite reductions, the previously reported strategies primarily employ transition-metal based coordination complexes as the active site models.[10,11,12] For example, an iron(II) complex $[N(afa^{Cy})_3Fe(OTf)](OTf)$ with amino-azafulvene ligand arms has been shown to reduce both NO_3^- and NO_2^- to afford NO.[10,11] Furthermore, an oxygen-deficient polyoxovanadate-alkoxide has been illustrated to reduce NO_3^- to NO *via* the intermediacy of NO_2^-.[13] Similarly, $[Cr(cyclam)Cl_2]^+$ has been described as an efficient electrocatalyst for NO_3^- reduction.[14] While most of the previously reported NO_3^- reduction routes lead to the selective generation of NO, electrocatalytic reduction of NO_3^- by $[Co(DIM)Br_2]^+$ supported by a redox-noninnocence ligand (DIM = 2,3-dimethyl-1,4,8,11-tetraazacyclotetradeca-1,3-diene) yields NH_3 as the sole reduction product.[15] Nevertheless, the approach of transition-metal mediated activation of NO_3^- is obscured due to (a) poor coordination ability of NO_3^- anion at the metal sites, (b) difficulty in multi-electron process aiming selective reduction product.[10] Herein we explore a proton-assisted metal-free route for NO_x^- reduction and hypothesize that electron-rich aromatics such as 1,3,5-trimethoxybenzene (TMB–H, **1a**) may serve as the sacrificial electron donor. Remarkably, nitrosation of TMB–H

[a] T. Sahana, A. Mondal, Anju B. S., Dr. S. Kundu*
School of Chemistry, Indian Institute of Science Education and Research Thiruvananthapuram (IISER–TVM),
Thiruvananthapuram – 695551, India.
E-mail: skundu@iisertvm.ac.in, skundu.chem@gmail.com

Supporting information for this article is given via a link at the end of the document.

10.1002/anie.202105723

follows an unusual route to yield oxoammonium salt $[(TMB)_2N^+{=}O][NO_3^-]$ (**2a**). Moreover, the ease of isolation and the relative stability of the subtle intermediate **2a** allow to report its detailed characterization including X-ray crystal structure and reactivity studies. In addition to the oxidative reactivity of oxoammonium salt **2a**, this report reveals that the hydrolysis of $[(TMB)_2N^+{=}O]$ (in **2a**) leads to the generation of ammonia in near quantitative yield.

Treatment of a colourless solution of 1,3,5-trimethoxybenzene (TMB–H, **1a**) in acetonitrile with $NaNO_x$ or $[^nBu_4N]NO_x$ in the presence of *para*-toluenesulfonic acid (PTSA) or trifluoroacetic acid (TFA) at room temperature leads to the generation of an intense blue species (**2a**) with a distinct absorption band centered at λ_{max} = 610 nm (Figures 2 and S1). Notably, a previous report on the electrophilic nitration of TMB–H (**1a**) and 1,3-dimethoxybenzene (DMB–H, **1b**) by Kochi *et al* indicated the generation of an "intense blue" species with the comparable absorption features.[16] However, the nature of the metastable species remained ambiguous. As the interactions of proton with NO_x^- anions are known to generate metastable nitrous acid (HONO) *in situ*,[17] we investigate the reaction of **1a** with a relatively stable nitrous acid model, namely ^{t}BuONO. Addition of ^{t}BuONO to a solution of **1a** in acetonitrile at room temperature under an inert atmosphere results in the generation of **2a** (Figure S2). Remarkably, monitoring the reaction of **1a** with ^{t}BuONO by UV-vis reveals that the generation of **2a** is ~30 folds faster in the presence of PTSA (Figure S3), thereby suggesting the involvement of nitrosonium cation (NO^+) prior to the generation of **2a**. Indeed, a reaction of **1a** with $[NO^+][BF_4^-]$ leads to the instantaneous formation of compound **2a**. Moreover, a reaction of TMB–H with NO_2 gas ($2NO_2 = N_2O_4 = [NO^+][NO_3^-]$) in dichloromethane leads to a rapid generation of compound **2a** in >95% isolated yield (Figure S4). X-ray crystal structure of compound **2a** renders the molecular structure of **2a** as an oxoammonium cation $[(TMB)_2N^+{=}O]$ with a nitrate (NO_3^-) counter anion (Figures 3 and S5). The N1–O4 bond distance in **2a** is found to be 1.248(3) Å, which is comparable to the analogous N–O distance (1.237(3) Å) in the previously reported temponium cation.[18] The sum of three angles at the oxoammonium nitrogen N1 is 360.02°, thereby indicating a sp^2 hybridized planar N-site in **2a**. High resolution mass spectrometric (HRMS) analysis on **2a**

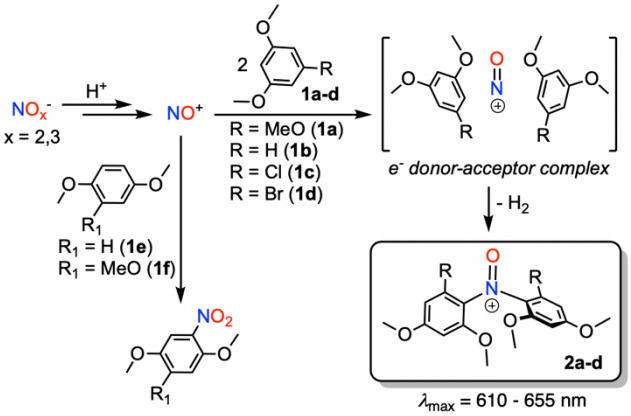

Figure 2. Reactions of methoxy-aryl compounds **1a-f** towards NO_x^-/H^+ and synthesis of oxoammonium salts **2a-d**.

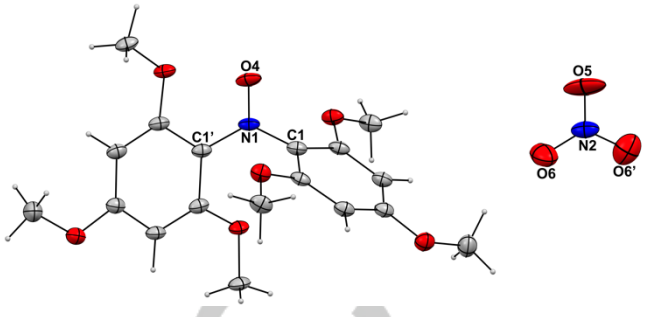

Figure 3. X-ray crystal structure (CCDC 2079167) of $[(TMB)_2N^+{=}O][NO_3^-]$ (**2a**) ellipsoids shown at 30% probability. Figure S5 shows selected metrical parameters.

exhibits a *m/z* peak at 364.1390 which can be attributed to the oxoammonium cation $[(TMB)_2N^+{=}O]$ (*calc. m/z* 364.1391) (Figure S6). Furthermore, FT–IR spectrum of **2a** shows distinct vibrational features at 1642 and 1384 cm^{-1}, thereby corroborating the respective presence of oxoammonium functional group and nitrate anion in **2a** (Figure S7).[19,20] The intense blue colour of **2a** is associated with the UV-vis absorption features centered at λ_{max}/nm ($\varepsilon_{max}/M^{-1}cm^{-1}$) = 390 (9200) and 610 (11070) (Figure S8). DFT calculation on $[(TMB)_2N^+{=}O]$ cation shows π-type interactions in HOMO and LUMO (Figure S12) and the lowest energy absorption feature at λ_{max} = 610 nm presumably originate due to the primary transition from HOMO to LUMO.[21] Thus, these results unambiguously reveal structural and spectroscopic signatures of a metastable diaryl oxoammonium cation (Figures S5-S12). Furthermore, the above-mentioned reactions illustrate that the reactions of TMB–H (**1a**) with various NO^+ sources conveniently provide an unusual diaryl oxoammonium species **2a** instead of commonly observed aromatic nitration yielding nitroaromatic. While the chemistry of aliphatic oxoammonium species is relatively well known,[19,22] structure-reactivity profile of analogous diaryl oxoammonium species remains elusive.[23]

Although the proton assisted transformation of NO_3^- to NO^+ presumably proceeds through a complex route, the activation of relatively unreactive NO_3^- has further been confirmed by employing ^{15}N–labelling experiments. Treatment of an acetonitrile solution of ^{15}N–enriched $Na^{15}NO_3$ with H^+/TMB–H affords $[(TMB)_2{}^{15}N^+{=}O][{}^{15}NO_3^-]$ (**2a**–^{15}N). ^{15}N NMR spectrum (*versus liq* NH_3) of **2a**–^{15}N depicts two distinct singlet ^{15}N-resonances at δ = 178 and 368 ppm (Figure S13), which can be attributed to the *N*-sites of oxoammonium cation and nitrate anion, respectively. Monitoring the reaction of **1a** with ^{t}BuONO or NO_2 gas in $CDCl_3$ by ^1H NMR exhibits a singlet at δ = ~4.2 ppm (Figure S14),[24] which can tentatively be assigned to the coformation of H_2 gas during the generation of oxoammonium species **2a**. Hence, we postulate that the interaction among two molecules of TMB–H with NO^+ leads to a transient 2:1 aromatic electron donor-acceptor complex, which dissociates to yield $[(TMB)_2N^+{=}O]$ and H_2 gas (Figures 1A and 2). Notably, structurally characterized analogous 2:1 aromatic electron donor-acceptor complex has been reported previously by Kochi *et al*.[25]

In contrast to the organic *O*–nitrite species, closely related organic *S*–thionitrites also known as *S*–nitrosothiols (*e.g.* ^{t}BuSNO) do not react with TMB–H (**1a**) under an inert atmosphere.

10.1002/anie.202105723

However, in the presence of oxygen, *S*-nitrosothiols react with **1a** to afford **2a**, which can be attributed to the reaction of TMB–H with the aerobically generated NO_2 ($2NO + O_2 = 2NO_2$). Thus, these findings reveal that *S*–nitrosothiols prefer S–N bond homolysis rather than heterolysis under the present reaction conditions. Moreover, the presence of PTSA or Lewis-acidic Zn^{2+} salts during the reactions of *S*–nitrosothiol with **1a** under the inert atmosphere do not afford the oxoammonium species **2a**.

To assess the generality of oxoammonium salt formation, we examined the reactivity of other differently substituted methoxy aryl derivatives towards ^{t}BuONO or NO_2 gas. 1,3-dimethoxybenzene (DMB–H, **1b**), 5-chloro-1,3-dimethoxybenzene (**1c**) and 5-bromo-1,3-dimethoxybenzene (**1d**) react with ^{t}BuONO or NO_2 gas similar to that of **1a** to provide respective oxoammonium salt derivatives (**2b**, **2c**, **2d**) with distinct intense colors. Moreover, UV-vis absorption studies reveal the presence of characteristic absorption features (λ_{max}) in the visible region as noticed for $[(TMB)_2N^+{=}O]$ (**2a**) (Figures S15, S21, S24). Notably, a Hammett plot analysis employing the lowest energy absorption feature (λ_{max}) ranging between 610 – 655 nm for the oxoammonium cations with the substituent variations of MeO, H, Cl, and Br shows a linear correlation with a positive slope (Figure S25). HRMS analyses on **2b**, **2c**, and **2d** affirm the formation of oxoammonium derivatives (Figures S18, S22, S26). While the instability of **2c** and **2d** limited the characterizations to UV-vis and HRMS, oxoammonium salt **2b** is sufficiently stable allowing NMR and X-ray crystallographic characterizations. X-ray crystal structure of **2b** exhibits a planar oxoammonium nitrogen (N1) with N1–O5 1.2587(16) comparable to that in **2a** (Figure S20). In contrast, reactions of 1,4-dimethoxybenzene (**1e**) and 1,2,4-trimethoxybenzene (**1f**) with ^{t}BuONO or NO_2 in dichloromethane solely lead to electrophilic aromatic nitration affording respective nitro-derivatives in near quantitative yields (Figure 2). Moreover, 3,5-dimethoxyphenol reacts with ^{t}BuONO or NO_2 in dichloromethane to yield a mixture of mono- and di-nitrophenol derivatives predominantly.[26]

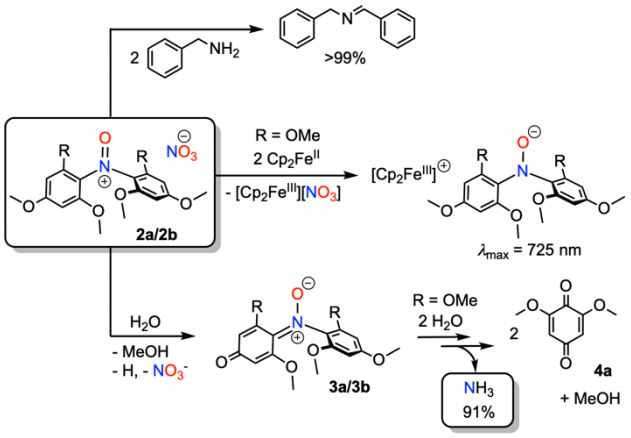

Figure 4. Reactivity of oxoammonium salts **2a/2b**. See Supporting Information Figure S48 for the proposed mechanism of NH_3 generation from **2a**.

Prompted by the isolations of oxoammonium salts **2a** and **2b**, we are inquisitive to investigate the reactivity of such species. While the oxidative reactivity of compound **2a** towards alcohol has found to be sluggish, **2a** oxidizes benzylamine to dibenzylimine in quantitative yield. Interestingly, reactions of benzylamine with a cocktail consisting of **1a**/**1b** + PTSA + $NaNO_x$ lead to a clean transformation to dibenzylimine (Figures 4 and Table S2). Notably, a control reaction of benzylamine with PTSA + $NaNO_x$ leads to a trace amount of dibenzylimine (Figure S32). To provide insights into the oxidative reactivity of **2a**, we investigate its reactions with $1e^-$ reducing agents such as thiophenol and ferrocene. Monitoring a reaction of **2a** with thiophenol (2.5 equiv) by UV-vis shows a decay of 610 nm feature and a growth of a new band at 725 nm with an isosbestic point at 665 nm (Figure 5A). GCMS analysis reveals the formation of disulfide (PhSSPh) in quantitative yield. ESI-MS analysis on the reaction mixture indicates the formation of TMB_2N–SPh (Figure S34), presumably *via* the intermediacy of a $2e^-$ reduced species TMB_2N–OH. Indeed, UV-vis monitoring of a reaction of **2a** with ferrocene (2.5 equiv) exhibits the formation of 725 nm species (Figure 5B), thereby suggesting direct $2e^-$ reduction of $[(TMB)_2N^+{=}O]$ without the involvement of any detectable aminoxyl $[(TMB)_2N{-}O\bullet]$ species. While the insights into the aliphatic oxoammonium mediated oxidation are relatively well documented,[19,22] this present study sheds light on the oxidative reactivity of diaryl oxoammonium species.

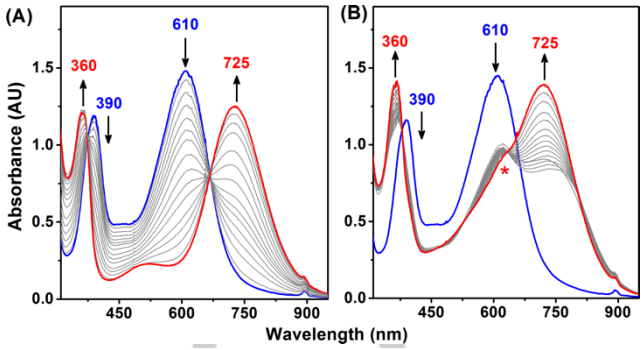

Figure 5. Changes in the UV-vis spectrum of **2a** (blue trace) in acetonitrile (2.0 mL, 0.15 mM) upon addition of 2.5 equivalents thiophenol (A) and ferrocene (B) at room temperature. * indicates the absorption feature at 620 nm originating due to the coformation of ferrocenium cation.

Illustrating the water sensitivity of oxoammonium cation, $[(TMB)_2N^+{=}O]$ (in **2a**) reacts with water and results in 2,6-dimethoxybenzoquinone (**4a**) in quantitative yield (Figure S36). Intriguingly, ^{1}H NMR spectrum of a crude reaction mixture consisting of **2a** (or **2a**–^{15}N) and water in d_6-dimethylsulfoxide exhibits a triplet (for **2a**) and a doublet (for **2a**–^{15}N) centered at δ = ~7.2 ppm ($^1J_{NH}$ = 50.3 Hz for ^{14}N and $^1J_{NH}$ = 71.8 Hz for ^{15}N),

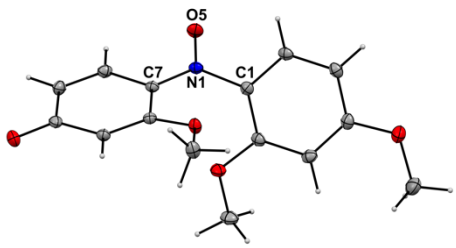

Figure 6. X-ray crystal structure of **3b** (CCDC 2079169), ellipsoid plotted at 30% probability. Figure S46 shows selected metrical parameters.

which can be corroborated to $^{14}NH_4^+$ and $^{15}NH_4^+$, respectively (Figure S37-S39).[27] Ammonia quantification by indophenol method provides 91% yield (Figures S40 and S41, Table S3).[28] Moreover, the ^{1}H NMR spectrum shows the coformation of methanol (Figure S37). Surprisingly, the reaction of $[(DMB)_2N^+=O]$ (**2b**) with water under analogous reaction conditions affords a stable compound **3b** (Figure S42). X-ray diffraction analysis reveals the molecular structure of **3b** and HRMS spectrum confirms the molecular composition (Figures 6, S43-S46). We postulate that a homologous intermediate **3a** may serve as a transient species for the reaction of **2a** with water prior to the release of ammonia. Indeed, HRMS analysis on **2a** in wet acetonitrile depicts a peak at *m/z* = 350.1231 (*calc. m/z* = 350.1234 for MH^+), which can be assigned to the intermediate species **3a** (Figure S47).

In summary, the present work illustrates proton-assisted activations of NO_x^- anions to NO^+, which undergoes unusual transformation to oxoammonium salts (**2a-d**) in the presence of electron-rich aromatics (**1a-d**). Thus, this report offers a convenient route for the generation oxoammonium species, an important intermediate in various oxidative transformations.[22] Moreover, a set of complimentary analyses on the metastable diaryl oxoammonium salts (**2a-d**) unfolds their spectroscopic and structural signatures. Illustrating the oxidative reactivity of oxoammonium species (**2a**), this work demonstrates $2e^-$ redox process in the presence of reducing agents such as benzylamine, thiols, and ferrocene. Remarkably, the hydrolysis of **2a** leads to the generation of ammonia in near quantitative yields. Thus, this work connects two extreme oxidation states of N, specifically N^{+V} in NO_3^- anion and N^{-III} in NH_3. Perhaps this may offer new opportunities for designing electrochemical routes targeting NO_x to NH_3 conversion.

Experimental Section

Experimental details are available in the Supporting Information.

Acknowledgements

S.K. gratefully acknowledges the Early Career Research Award (ECR/2017/003200) from SERB. Authors are also thankful to IISER-TVM for financial supports.

Keywords: Nitrogen-oxides • Nitrosonium • Oxoammonium • Ammonia • Electron rich aromatics

[1] X. Zhang, B. B. Ward, D. M. Sigman, *Chem. Rev.* **2020**, *120*, 5308–5351.
[2] C. Sparacino-Watkins, J. F. Stolz, P. Basu, *Chem. Soc. Rev.* **2014**, *43*, 676–706.
[3] L. B. Maia, J. J. G. Moura, *Chem. Rev.* **2014**, *114*, 5273–5357.
[4] J. O. Lundberg, M. T. Gladwin, A. Ahluwalia, N. Benjamin, N. S. Bryan, A. Butler, P. Cabrales, A. Fago, M. Feelisch, P. C. Ford, et al., *Nat. Chem. Biol.* **2009**, *5*, 865–869.
[5] P. G. Wang, M. Xian, X. Tang, X. Wu, Z. Wen, T. Cai, A. J. Janczuk, *Chem. Rev.* **2002**, *102*, 1091–1134.
[6] N. Hogg, *Annu. Rev. Pharmacol. Toxicol.* **2002**, *42*, 585–600.
[7] L. Batt, K. Christie, R. T. Milne, A. J. Summers, *Int. J. Chem. Kinet.* **1974**, *6*, 877–885.
[8] M. R. Talipov, Q. K. Timerghazin, *J. Phys. Chem. B* **2013**, *117*, 1827–1837.
[9] A. Dahiya, A. K. Sahoo, T. Alam, B. K. Patel, *Chem. Asian J.* **2019**, *14*, 4454–4492.
[10] C. L. Ford, Y. J. Park, E. M. Matson, Z. Gordon, A. R. Fout, *Science* **2016**, *354*, 741–743.
[11] E. M. Matson, Y. J. Park, A. R. Fout, *J. Am. Chem. Soc.* **2014**, *136*, 17398–17401.
[12] A. Mondal, K. P. Reddy, J. A. Bertke, S. Kundu, *J. Am. Chem. Soc.* **2020**, *142*, 1726–1730.
[13] B. E. Petel, E. M. Matson, *Chem. Commun.* **2020**, *56*, 555–558.
[14] S. E. Braley, D. C. Ashley, E. Jakubikova, J. M. Smith, *Chem. Commun.* **2020**, *56*, 603–606.
[15] (a) S. Xu, D. C. Ashley, H.-Y. Kwon, G. R. Ware, C.-H. Chen, Y. Losovyj, X. Gao, E. Jakubikova and J. Smith, *Chem. Sci.* **2018**, *9*, 4950–4958. (b) S. Xu, H.-Y. Kwon, D. C. Ashley, C.-H. Chen, E. Jakubikova and J. M. Smith, *Inorg. Chem.* **2019**, *58*, 9443–9451.
[16] S. Sankararaman, W. A. Haney, J. K. Kochi, *J. Am. Chem. Soc.* **1987**, *109*, 5235–5249.
[17] M. A. Kamboures, J. D. Raff, Y. Miller, L. F. Phillips, B. J. Finlayson-Pitts, R. B. Gerber, *Phys. Chem. Chem. Phys.* **2008**, *10*, 6019–6032.
[18] S. Stefanom, F. Belaj, T. Madl, R. Pietschnig, *Eur. J. Inorg. Chem.* **2010**, *3*, 289–297.
[19] M. Shibuya, Y. Osada, Y. Sasano, M. Tomizawa, Y. Iwabuchi, *J. Am. Chem. Soc.* **2011**, *133*, 6497–6500.
[20] T. Chattopadhyay, B. S. Anju, S. Gupta, S. Ananya, J. A. Bertke, S. Kundu, *Dalt. Trans.* **2019**, *48*, 7085–7089.
[21] See supporting information for the details of DFT calculations.
[22] B. L. Ryland, S. S. Stahl, *Angew. Chem. Int. Ed.* **2014**, *53*, 8824–8838.
[23] V. A. Golubev, V. D. Sen, *Russ. J. Org. Chem.* **2013**, *49*, 1143–1149.
[24] H. Fujiwara, J. Yamabe, S. Nishimura, *Chem. Phys. Lett.* **2010**, *498*, 42–44.
[25] R. Rathore, S. V. Lindeman, J. K. Kochi, *Angew. Chem. Int. Ed.* **1998**, *37*, 1585–1587.
[26] HRMS analysis on a freshly prepared crude sample obtained from the reaction of 3,5-dimethoxyphenol and ^{t}BuONO shows *m/z* at 336.1073 (*calc. m/z* 336.1078), which can be attributed to the formation of corresponding oxoammonium salt. The detailed characterization of the oxoammonium salt, however, was not possible due to the poor yield as well as its instability.
[27] H. S. Kim, J. Choi, J. Kong, H. Kim, S. J. Yoo, H. S. Park, *ACS Catal.* **2021**, *11*, 435–445.
[28] A. C. Nielander, J. M. McEnaney, J. A. Schwalbe, J. G. Baker, S. J. Blair, L. Wang, J. G. Pelton, S. Z. Andersen, K. Enemark-Rasmussen, V. Čolić, et al., *ACS Catal.* **2019**, *9*, 5797–5802.
[29] CCDC 2079167 (**2a**), CCDC 2079168 (**2b**), and CCDC 2079169 (**3b**) contain the supplementary crystallographic data for this paper. These data can be accessed free of charge from The Cambridge Crystallographic Data Centre.

10.1002/anie.202105723

WILEY-VCH

COMMUNICATION

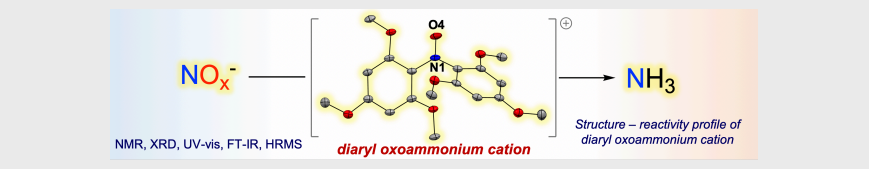

Proton-assisted transformations of nitrogen-oxyanions (NO_x^-) in the presence of 1,3,5-trimethoxybenzene (TMB-H) leads to an elusive diaryl oxoammonium species $[TMB_2NO]^+$. In addition to the $2e^-$ oxidative chemistry of $[TMB_2NO]^+$ towards oxidizable substrates, this report illustrates water promoted decomposition of $[TMB_2NO]^+$ affording ammonia.

*Tuhin Sahana, Aditesh Mondal, Anju B. S., and Subrata Kundu**

Page No. – Page No.

Metal-free Transformations of Nitrogen-oxyanions to Ammonia *via* Oxoammonium Salt